IOP Publishing | Royal Swedish Academy of Sciences Physica Scripta
Phys. Scr. 92 (2017) 114007 (8pp) https://doi.org/10.1088/1402-4896/aa90a3

Investigation of electron beam lithography effects on metal–insulator transition behavior of vanadium dioxide

H Yuce[1], H Alaboz[1], Y Demirhan[1], M Ozdemir[1,2], L Ozyuzer[1,2] and G Aygun[1]

[1] Department of Physics, Izmir Institute of Technology, 35430 Urla, Izmir, Turkey
[2] Teknoma Technological Materials Ltd, 35430 Urla, Izmir, Turkey

E-mail: ozyuzer@iyte.edu.tr

Received 26 April 2017, revised 25 September 2017
Accepted for publication 3 October 2017
Published 25 October 2017

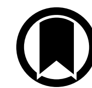

Abstract
Vanadium dioxide (VO_2) shows metal–insulator phase transition at nearly 68 °C. This metal–insulator transition (MIT) in VO_2 leads to a significant change in near-infrared transmittance and an abrupt change in the resistivity of VO_2. Due to these characteristics, VO_2 plays an important role on optic and electronic devices, such as thermochromic windows, meta-materials with tunable frequency, uncooled bolometers and switching devices. In this work, VO_2 thin films were fabricated by reactive direct current magnetron sputtering in O_2/Ar atmosphere on sapphire substrates without any further post annealing processes. The effect of sputtering parameters on optical characteristics and structural properties of grown thin films was investigated by SEM, XRD, Raman and UV/VIS spectrophotometer measurements. Patterning process of VO_2 thin films was realized by e-beam lithography technique to monitor the temperature dependent electrical characterization. Electrical properties of VO_2 samples were characterized using microprobe station in a vacuum system. MIT with hysteresis behavior was observed for the unpatterned square samples at around 68 °C. By four orders of magnitude of resistivity change was measured for the deposited VO_2 thin films at transition temperature. After e-beam lithography process, substantial results in patterned VO_2 thin films were observed. In this stage, for patterned VO_2 thin films as stripes, the change in resistivity of VO_2 was reduced by a factor of 10. As a consequence of electrical resistivity measurements, MIT temperature was shifted from 68 °C to 50 °C. The influence of e-beam process on the properties of VO_2 thin films and the mechanism of the effects are discussed. The presented results contribute to the achievement of VO_2 based thermochromic windows and bolometer applications.

Keywords: vanadium dioxide, metal insulator transition, e-beam lithography, magnetron sputtering

(Some figures may appear in colour only in the online journal)

1. Introduction

Transition metal oxides have been investigated widely due to their peculiar electrical and optical properties. Vanadium dioxide (VO_2) indicates a reversible metal insulator transition (MIT) at ∼68 °C [1, 2]. It has been reported that MIT behavior of VO_2 strongly varied in wide range with crystal quality, grain size, grain boundaries and defects related to self-doping and the other factors [3, 4]. While VO_2 has monoclinic crystal structure with insulator phase at below the MIT temperature (T_{MIT}), the material has tetragonal rutile crystal structure with metallic phase at above T_{MIT} [5, 6]. During the transition, the change in the volume of VO_2 crystal is around 1%–2% [7]. In insulator phase, the energy bandgap of VO_2 is around 0.65 eV [8]. There have been two views on the origin of MIT in VO_2; Peierles transition and Mott–Hubbard transition. Peierles transition arises due to the change in crystal structure, and Mott–Hubbard transition takes places due to electron-electron correlations [9]. MIT in VO_2 can be induced by heating [10], doping [11, 12], ion bombardment [13] and UV light [14].

 © 2017 IOP Publishing Ltd Printed in the UK

Table 1. Deposition parameters and morphology of VO_2 samples.

Sample	Reactive oxygen ratio (%)	Deposition time (min)	Average grain size (nm)	Thickness (nm)	Electrical properties
A	2.00	45	NA	310	MIT
B	2.00	22.5	<20	120	Non-transition (metallic)
C	2.25	22.5	NA	125	MIT
D	2.50	22.5	150	124	Non-transition (insulator)
E	3.00	22.5	150	127	Non-transition (insulator)

Insulator VO_2 has high transmittance whereas metallic VO_2 becomes opaque to near-IR radiation [15, 16]. MIT behavior of VO_2 is not only accompanied by significant change in infrared transmittance but also sharp change in resistivity. The transition takes place in approximately 80 fs, which is useful property for switching applications [17]. Moreover, MIT in VO_2 exhibits hysteresis behavior which can be tuned. These characteristics can be useful in many areas of optics and electronics, such as thermochromic windows [18, 19], tunable frequency meta-materials [20], detectors [21–24] and switching devices [25, 26]. Sensor applications require negligible hysteresis with high resistance drop during phase transition while the storage type devices require relatively large hysteresis [27].

There are various techniques to fabricate VO_2 films, such as pulsed laser deposition [28], chemical vapor deposition [29], atomic layer deposition [30], spray pyrolysis [31] thermal oxidation [32], sol-gel method [33] and magnetron sputtering [34, 35]. Being the most suitable technique in terms of large area growth, uniform deposition and high crystal quality [36], magnetron sputtering technique has advantageous in many respects to the others techniques.

Since it has been a challenging task to grow high quality VO_2 thin films, various substrates have been used as seen from the literature [15, 37]. The microstructure of deposited VO_2 thin films depends on lattice matching and surface energy of the substrates. Although silicon substrates are relatively cheaper and widely used in microelectronics, it is quite challenging to deposit high quality VO_2 films due to unavailability of its native oxide layer on the silicon substrates [37]. However, the sapphire substrates are commonly used for achieving high quality VO_2 thin films due to the fact that it has high thermal conductivity compared to the other ones.

In this study, VO_2 thin films were successfully grown on c-cut sapphire without any post annealing processes. The structural, optical and electrical properties of these grown thin films were investigated. The grown VO_2 films were patterned by e-beam lithography for the electrical measurements. The effect of structure size, patterning process on resistivity and MIT characteristics of VO_2 thin film were investigated. It is observed that e-beam patterned stripes with narrowed width (e.g. high aspect ratio ranging from 44 to 220) have peculiar properties. These will be discussed in detail in results and discussion part. The main outcome of this study is highly important that T_{MIT} was decreased from 68 °C to 50 °C as a result of e-beam lithography processing.

2. Experimental procedure

VO_2 thin films were deposited on c-cut sapphire (Al_2O_3 (0001)) using high purity (99.95%) vanadium (V) target by DC magnetron sputtering technique [38, 39]. Substrates were cleaned with acetone and DI water by means of ultrasonic cleaner. The vacuum chamber was evacuated to a base pressure of 1.2×10^{-6} mbar and the substrate was kept at 550 °C during deposition. In order to get rid of any contaminations of target's surface, 10 min pre-sputtering was performed on the target prior to deposition. VO_2 thin films were grown under 8.5×10^{-3} mbar of O_2 and Ar mixed gas pressure environment and 50 W of sputtering power. The substrates were rotated at 15 rpm in order to improve the uniformity of the film during the deposition process. Oxygen gas ratio of the sputtered thin films was varied in order to investigate the growth conditions of VO_2 thin films having sharp resistivity changes at T_{MIT}. Sample deposition parameters and the properties of the discussed films can be seen in table 1. In our experiments, firstly 310 nm VO_2 (named sample A) was grown on sapphire substrate during 45 min. According to analysis results, high quality VO_2 with the high change in resistivity depending on the temperature was observed. After that, in order to obtain thinner VO_2 film, we reduced deposition time from 45 to 22.5 min. Therefore, we obtained 125 nm vanadium oxide thin films with various unexpected phase at different oxygen concentrations. According to optimized parameters of the sample A, deposition time was reduced to 22.5 min at the same oxygen concentration (2.00%), and we deposited 125 nm VO_x with 2.00% oxygen rate (named sample B). For sample B, MIT was not observed. Due to that, oxygen concentration was increased up to 3.00% (named sample C for 2.25% O_2, sample D for 2.50% O_2, sample E for %3.00 O_2) with 22.5 min deposition time. However, for 125 nm VO_x thin films, high quality VO_2 thin film like sample A could not be obtained. 125 nm grown VO_x thin films except sample C did not exhibit MIT. As considering all grown films, only sample A and sample C show a transition. When especially electrical analysis results were examined, it is clear that sample A is more quality with high changing resistivity rate than sample C.

Structural and morphological properties of the films were characterized by field emission scanning electron microscopy (FE-SEM, Philips Quanta) equipped with energy dispersive spectroscopy (EDS, Oxford X-act). X-ray diffractometry (XRD, Philips PANanalytical X'Pert System) was used for the structural properties of the grown VO_2 thin films. The

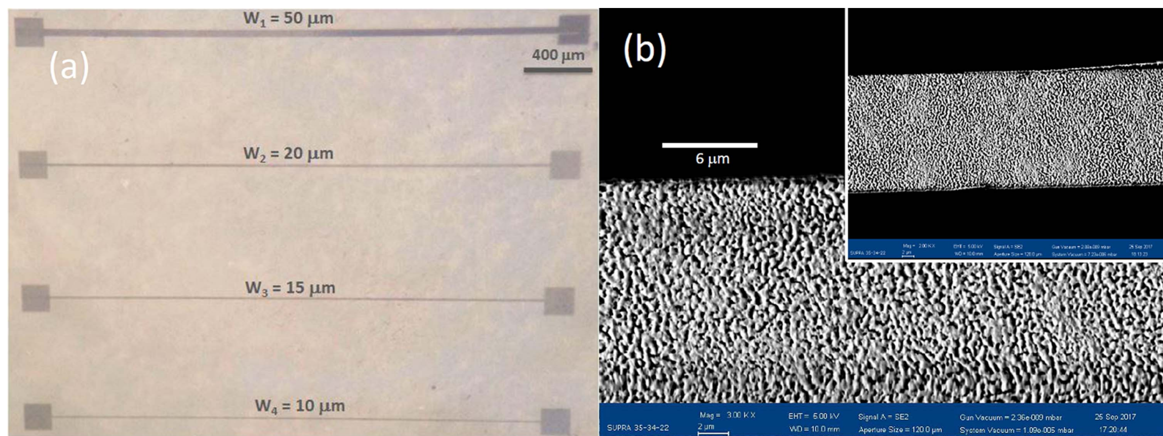

Figure 1. In order to investigate e-beam effect on VO_2 thin films, the VO_2 strips with varied dimensions were designed and fabricated. (a) The optical image of e-beam patterned VO_2 thin film (sample A, 310 nm thickness) strips with 50, 20, 15 and 10 μm strip widths (W) and 2.2 mm strip length is given. (b) SEM image of 20 μm width strip edge. The black region is sapphire. The inset shows the full width of the strip which corresponds to 20 μm.

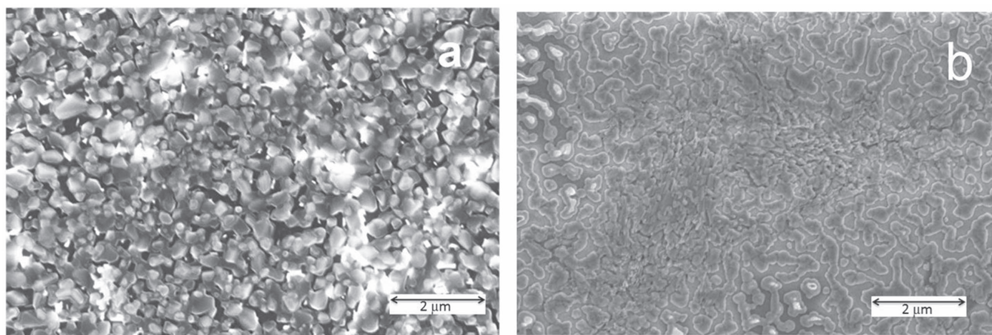

Figure 2. Field emission scanning electron microscope (SEM) images of 310 nm VO_2 thin film (sample A) (a) and 125 nm VO_2 thin film (sample C) (b) with 2 μm length scale bars. (Among all grown vanadium oxide thin films given in table 1, sample A and sample C have both shown MIT.)

XRD measurements were performed from 10° to 80° for 2θ using Cu K_α radiation ($\lambda = 1.5406$ Å) with step size of 0.04° and time step of 1 s. Optical transmittance spectra of samples at normal incidence were taken between 200 and 1200 nm using spectrophotometer (UV/VIS Spectrophotometer, Perkin Elmer) with a precisely controlled homemade heating mechanism. The thickness of the grown thin films was measured by a surface profilometer (Veeco DEKTAK 150). Raman measurements were taken by a confocal Raman spectroscopy (Scientific Instruments). The resolution of the Raman measurements was 2.0 cm^{-1}. Argon laser with 514 and 633 nm excitation wavelengths having 120 mW (514 nm laser) and 20 mW (633 nm laser) power were used for the Raman analysis.

Deposited high quality VO_2 thin films were patterned by e-beam lithography (Raith e-line e-beam lithography system) to investigate the effects of e-beam on MIT characteristics of aforementioned films. For this purpose, the VO_2 films were coated with AZ5214 photoresist at 3000 rpm for 50 s. Photoresist coated films were heat treated for 30 min in a furnace kept at 90 °C. After the film was patterned by e-beam, it was exposed to ultraviolet light (OAI Mask Aligner) for 7 s. Later, it was put in developer solution and rinsed with deionized water. Followed by hard bake process at 120 °C, Ar ion milling was performed. The samples were water cooled during etching of VO_2 to create strips. Remaining photoresist was stripped away with acetone at the last step of the patterning process [40, 41]. Final structure of shaped VO_2 stripes and a representative SEM picture were given in figure 1. The discussion of the images were deferred to a later part of this paper.

Electrical measurements of VO_2 samples were done between 30 °C and 100 °C with usage of microprobe station (Janis Microprobe Station). A Labview controlled computer program was used to record the measurements done by a Keithley sourcemeter.

3. Results and discussions

3.1. Structural properties

Surface morphologies of the grown VO_2 thin films having different O_2/Ar flow rates and deposition durations were investigated using SEM (figure 2). There are many variables such as substrate, growth temperature, deposition rate and sputtered ion energy affecting the quality of the grown vanadium oxide films. In this study, we investigated two

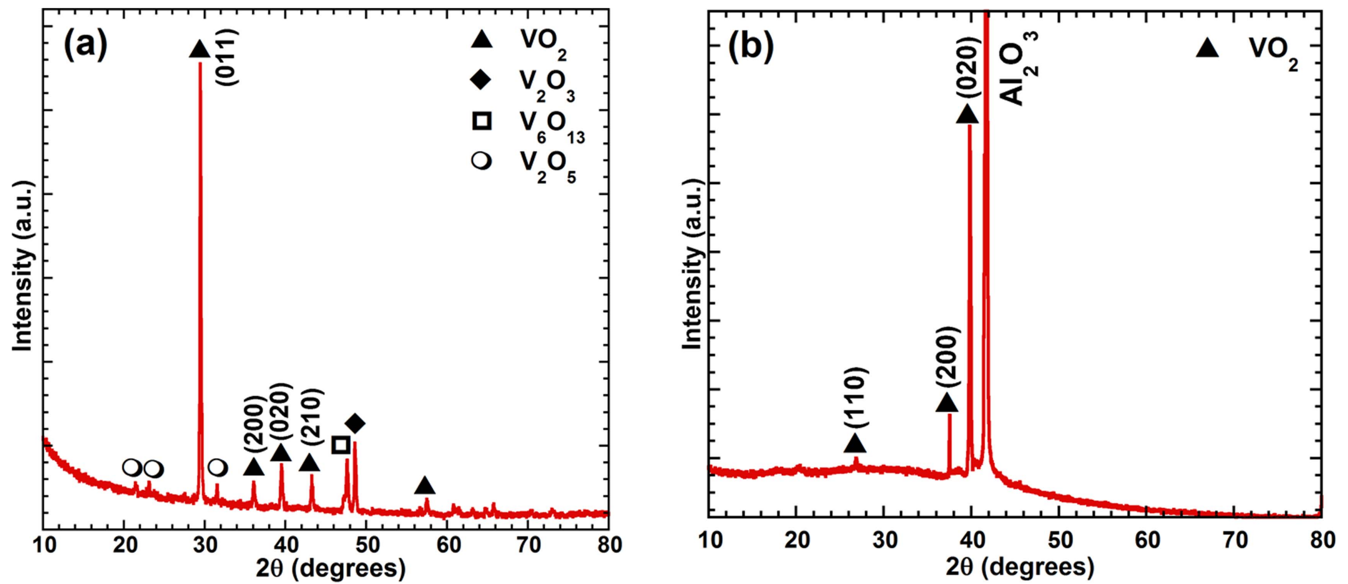

Figure 3. XRD spectrum of sample A (a) and sample C (b) which shows MIT behavior. Here, it is seen that sample A −310 nm film thickness with 2.00% oxygen concentration- exhibits high intensity VO_2 diffraction peak. However, XRD diffraction peaks of sample C −125 nm film thickness with 2.25% oxygen concentration—belong to VO_2 are at lower intensity.

parameters, namely oxygen concentration in grown vanadium oxide films and the thickness of the films. These two variables in our experiments affect grain size and surface morphology of the thin films. As shown in table 1, sample A and C exhibit MIT among deposited thin films.

Figure 2 shows SEM images of samples A and C. While sample A has small grains (figure 2(a)), sample C has meander like structure (figure 2(b)). It is concluded that increasing deposition time and decreasing oxygen concentration of the films convert meander like grains to small grains. This effect can be explained with the diffusion and migration of adsorbed atoms; increasing deposition time gives additional time to adatoms for diffusion and migration on the substrate surface which is essential for nucleation and growth [42].

The XRD patterns of as grown thin films at different O_2 flow rates and growth duration were collected for 2θ between 10° and 80°. There are two important peaks observed at ∼29° and 39° related to VO_2 as seen in figure 3(a). These can be assigned to (011) and (020) diffraction peaks [42]. Since the film is quite thin for sample C, a strong peak at $2\theta \sim 41°$ is detected belonging to sapphire substrate [43] as shown in figure 3(b). According to XRD results, the films consist of mixed phases, i.e. VO_2, V_2O_3, V_2O_5 and V_6O_{13} [43, 44]. It can be understood from the XRD peaks that 2.00% oxygen to argon ratio is a reasonable choice to grow 310 nm thick vanadium oxide films in the form of mainly VO_2 phase. In addition, in case of thickening the grown film, the orientation of vanadium oxide crystal changes compared to substrate orientation, and this leads to consist of more polycrystalline structure as in sample A. Due to the change in crystal orientation depending on the film thickness, the peaks which are the highest intensity belong to sample A and C are different from each other.

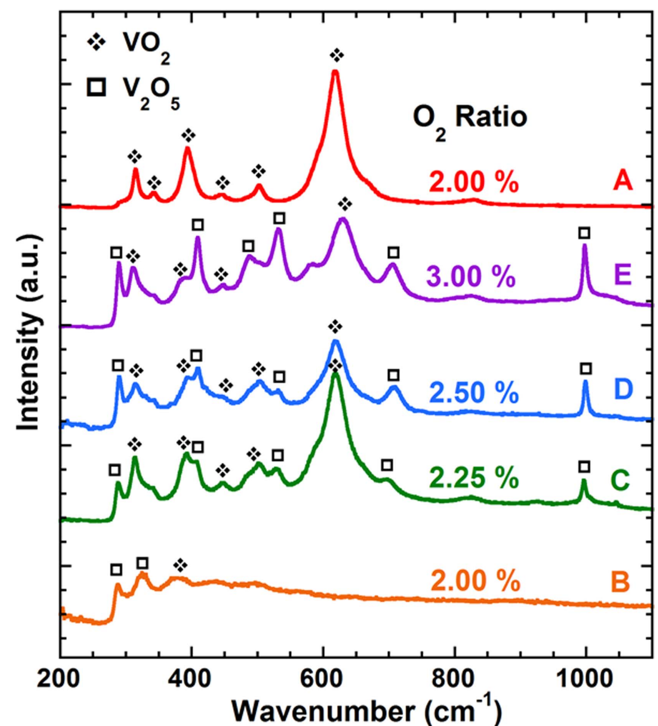

Figure 4. Raman spectra of thin films deposited at different O_2/Ar flow ratios. Note that sample A is thicker than the rest of the samples. According to the Raman spectra of sample A and sample B, main observed vanadium oxide Raman modes are disappeared with decreasing film thickness. Also, in case of decreasing O_2/Ar flow ratio, the grown vanadium oxide thin films with the same thickness (sample B, C, D and E) exhibit more metallic properties.

Raman microscopy analyses were carried out at room temperature for each sample in order to investigate the oxygen flow ratio effects on the phases of vanadium oxide films (figure 4). In order to prevent phase transition due to heating effects during the measurement, laser intensity was

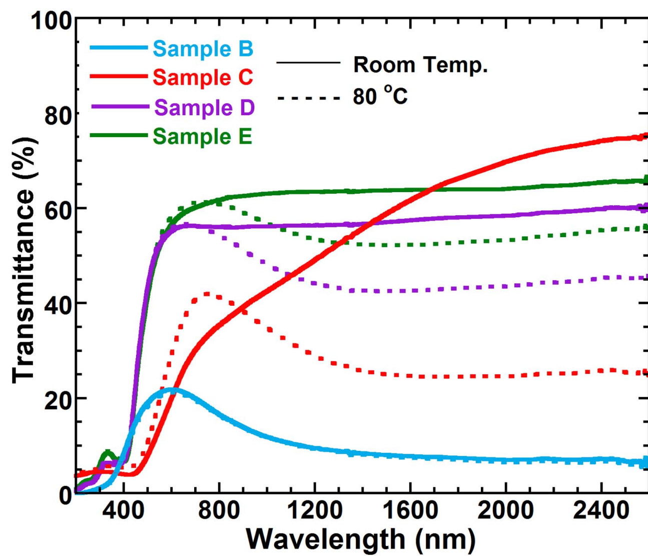

Figure 5. Optical properties of deposited VO_2 thin films with different oxygen flow ratios at room and above transition temperatures. Note that solid lines correspond to room temperature measurement and dashed lines for 80 °C ones.

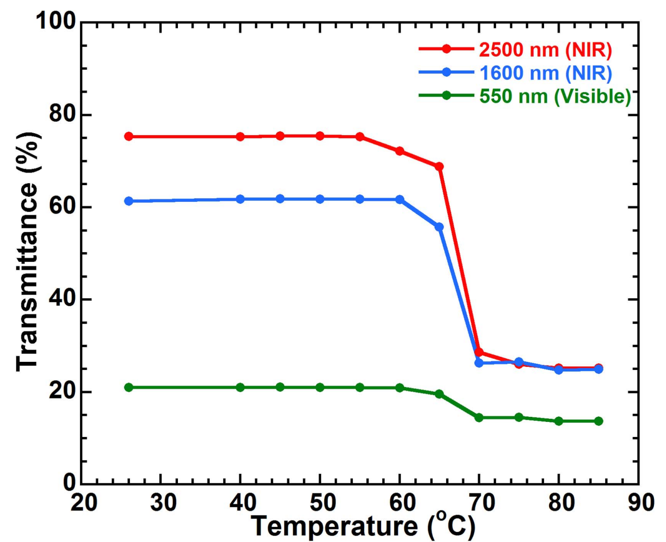

Figure 6. Temperature dependent transmission change is seen for various wavelengths in sample C.

minimized to its lowest possible value. Raman analysis show that VO_2 and V_2O_5 coexist in grown thin films except for sample A. Raman peaks detected at 313, 342, 392, 445, 502 and 617 cm^{-1} correspond to VO_2 phase as reported in the literature [45]. The main V–V band at 617 cm^{-1} belongs to VO_2 phase. Besides VO_2 peaks, the detected signals at 288, 408, 488, 530, 704 and 997 cm^{-1} correspond to V_2O_5 characteristic peaks [46]. The highest Raman intensities belonging to VO_2 phase with a lower V_2O_5 intensity mode are detected for sample C grown at 2.25% oxygen ratio compared to the other ones having the same thickness. As a result, it can be concluded that 2.25% oxygen ratio for 125 nm thick film includes more abundant peaks corresponding to strong vibrational modes of VO_2 phase. As increasing O_2 ratio from 2.25% to 3.00%, the intensity of V_2O_5 phase increases while that of VO_2 phase decreases. The Raman peak at 285 cm^{-1} is assigned to V_2O_5 phase of sample B [46]. Also, the broad peak at around 320 cm^{-1} could be belong to amorphous V_2O_5 [47]. For sample B, there is another broad peak at around 386 cm^{-1} which is shifted by $\sim$6 cm^{-1} compared to the Raman peak of sample A at 392 cm^{-1}. This Raman shift may be related to chemical bond of the molecule. These results are supported by XRD analysis that when the oxygen gas ratio increases above 2.25%, the percentage of VO_2 decreases while V_2O_5 phase increases.

3.2. Optical properties

Transmittance spectra measured at room temperature and 80 °C of grown VO_2 thin films (samples B, C, D and E) grown under different O_2 flow rates are shown in figure 5. Due to higher thickness of sample A (see table 1), transmittance measurements of all samples are not comparable. Therefore, the transmission spectrum of sample A was not set in this graph. Due to phase transition, the transmittance of the films decreases in near-IR region above MIT temperature. As it is clearly seen from the plots, VO_2 thin films show high optical transmission in their insulating state, i.e. at room temperature, while low optical transmission in their metallic state in IR region above MIT temperature, namely 80 °C. Moreover, transmittance change was not observed in the film grown under 2.00% O_2 (sample B) flow rate. Since the as grown film is already in metallic phase, transmission at all temperatures, as expected, is low in IR region corresponding to the metallic case behavior. For grown thin films with 2.50%–3.00% O_2 ratio, the transmittance variation rates are almost the same, being around 8%–15%. As it can be clearly seen in figure 5, VO_2 thin film grown under 2.25% oxygen ratio had the MIT, and showed the highest change in transmittance at IR region. Above transition temperature, VO_2 has metallic phase resulting in an increment of electron concentration in the conduction band.

Figure 6 indicates the temperature dependent transmittance of deposited 125 nm VO_2 thin films grown under 2.25% oxygen flow ratio at the wavelengths of 1600 and 2500 nm for near infrared and 550 nm for visible regions. In visible region, transmittance varies 7% with temperature, and it is about 21% at low temperatures. In addition, transmittance change at MIT region is around 36% for 1600 nm and 50% for 2500 nm wavelength. It is concluded that transmittance of insulator VO_2 phase is higher for 2500 nm than that of 1600 nm wavelength.

3.3. Electrical properties

It is known that mixed phases of vanadium oxide systems need to be optimized in terms of sputtering parameters to yield high quality pure VO_2 phase. One of the most important properties that determine film quality is the resistivity drop at T_{MIT}. It is indicated that the change in resistivity depends on uniformity of the film [48], strain, grain size and boundaries [3, 4, 49]. Epitaxially grown VO_2 films are known to be the

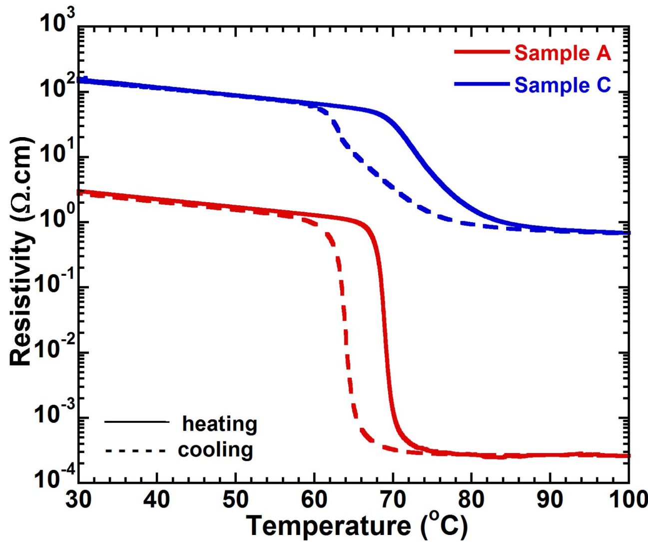

Figure 7. Thickness dependence of resistivity change across the MIT for sample A (310 nm) and C (125 nm) which are square samples.

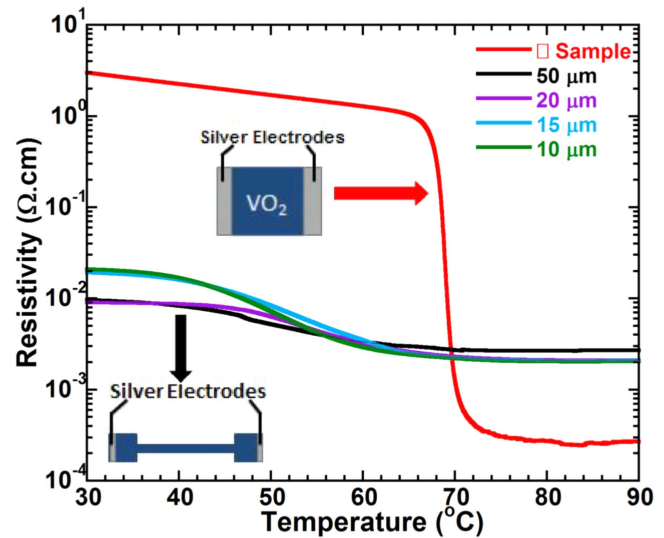

Figure 8. Temperature dependence of resistivity (during heating) for square sample A and the stripes with various widths.

best qualified films, and they exhibit resistivity changes an order of four at transition temperature [50]. Their hysteresis width of temperature changes from 0.5 °C to 2 °C [51]. Recent studies support that resistivity changes in high quality VO_2 films is about 10^4 for magnetron sputter deposited VO_2 films [26]. In our experiments, the sputtering conditions were optimized to obtain VO_2 thin films having 10^4 resistivity drop at T_{MIT}.

Figure 7 shows the resistivity of these films in the measurement range between 30 °C and 90 °C. The size of square samples was 4 mm × 4 mm. Note that the square samples were cut from large VO_2 grown substrate, and silver electrodes were deposited. Square samples were not exposed to any e-beam process. It is clearly seen that the resistivity of sample A at transition temperature decreases more than 10^4 of magnitude. T_{MIT} is about 68 °C, and the hysteresis loop width is about 4 °C for sample A, which are quite good values for DC sputtered VO_2 thin films [52]. In addition, it is observed that resistivity change across transition decreases by a factor of 10^2 for sample C. Therefore, it can be concluded that the films including high oxygen concentration with mixed phases show less resistivity change at transition temperature. The deposition time is an important factor to observe MIT in VO_2. When deposition time decreases to 22.5 min from 45 min, grown films are exposed to high temperature with 550 °C for less time. This leads to reduce the reactions of scattered V atoms with oxygen atoms. In this instance, instead of VO_2, other vanadium oxide phases take place. Because of the reason, Sample B could not exhibit MIT at nearly 68 °C. Sample B exhibits more metallic properties compared to the other grown vanadium oxide thin films due to exposing lower reactions with oxygen atoms. For the other samples, in case of increasing oxygen concentration (from 2.00% to 3.00%) with 22.5 min deposition time, it is necessary that new deposition parameters like deposition pressure should be determined in order to observe MIT. Under sample D and sample E fabrication conditions, there is more than enough oxygen present to react with V atoms. The excess of oxygen concentration leads to coexist unexpected secondary phases and VO_2 phase. Thus, these secondary phases prevent or reduce MIT in grown vanadium oxide thin film. Due to the excess of the oxygen concentration, sample D and sample E do not exhibit MIT properties.

Figure 8 shows temperature dependence of resistivity for a square sample and the e-beam lithography patterned VO_2 stripes. Note that the square sample is not patterned and measured as grown. The square sample is shown as an inset picture of figure 8, whereas the optical microscopy and SEM images of stripes can be seen in figure 1. The length of the stripes was 2.2 mm and the widths of the stripes were changed from 10 to 50 μm. Therefore, aspect ratios were ranging from 220 to 44. It has been observed that the resistivity of VO_2 stripes decreased down to around 10^{-2} Ω cm at room temperature (figure 8). It can be also seen that the T_{MIT} shifted to about 50 °C. On the other side, the resistivity drop was only one order for the stripes at T_{MIT}. As a summary, when the electrical properties of the square sample are compared to those of stripes, three distinct changes occur: (i) the resistivity value at room temperature decreases, (ii) resistivity changes at MIT get smaller, (iii) T_{MIT} shifts to 50 °C from 68 °C which is getting closer to room temperature, and (iv) the resistivity value at room temperature increases. These variations could be related to the e-beam patterning processes of the stripes. We investigated the influence of soft bake, developer and hard bake on the electrical properties of VO_2 films. However, there was not any change in electrical results for VO_2. The stripes of VO_2 films were exposed to electrons with 10 keV energy during e-beam lithography process held around 1.3×10^{-6} Torr vacuum. Under this circumstance, electron beam could affect the structure of grown VO_2 thin film. During e-beam lithography process, applied electron current leads to local heating on the surface of the film. In case of taking place local heating in high vacuum ambiance, a number of oxygen might release from VO_2 thin film.

Therefore, the reduction in oxygen concentration of grown VO2 film leads to consist of secondary phase which are in metallic phase of vanadium oxide compounds. Since the electrons prefer low resistance paths, it is reasonable that we get low resistivity at room temperature for e-beam patterned samples. In contrary to this, the secondary phases increase the resistance above T_{MIT} for patterned samples. As a result, we observe distinct properties of VO_2 stripes produced after e-beam lithography processes than those of square sample. Moreover, as we know from the literature studies, since the MIT in V_2O_3 and V_6O_{13} occurs, respectively, at –105 °C [53] and –123 °C [54], they are in metallic phases of vanadium oxide at the temperatures of our measurement region. In order to create patterned VO_2 structures, there are various methods, such as lift-off process [55]. Compared to their works which include lift-off method, we examined electron beam effect on VO_2 thin film. In order to create patterned vanadium oxide stripes, VO_2 thin film was shaped by electron beam lithography. In our works, during electron beam writing on VO_2 thin film, the film was exposed to electron beam with 10 keV energy. Our works show that electron beam lithography leads to decrease the change in resistivity of patterned stripes compared to VO_2 thin film. In order to give shape to VO_2 film, because of the negative effect of electron beam lithography, lift-off process could be better option for now. In this case, new research and studies will be required in order to prevent negative effect of electron beam lithography. Because electron beam lithography provides significant advantages in terms of its high resolution property for nanotechnology. Furthermore, SEM picture in figure 1(b) demonstrates large roughness of the sample. While the details of picture reveals grains as given in figure 2(a), figure 1(b) could be between figures 2(a) and (b) in terms of the surface morphology. So this change could be caused by e-beam influence on stripes.

3.3.1. Raman analysis results of patterned vanadium oxide stripes. Because of the nano-stripes, we are not able to look at XRD study to find crystal structure of patterned stripes. Furthermore, XPS studies cannot obtain local data from these stripes. On the other hand, we analyzed vanadium oxide stripes by confocal Raman spectroscopy, and Raman analysis results is shown in figure 9.

Due to strong resonance effect, in order to observe the Raman peaks at 192 and 222 cm^{-1}, 633 nm laser is better than 514 nm one. Because of this, in order to observe all phonon modes and prevent weak signals, 633 nm laser was used for Raman analysis of patterned samples. In figure 9, the vibration bands of VO_2 were observed by the peaks at 192, 222, 260, 306, 337, 386, 442, 497 and 613 cm^{-1}. These peaks are consistent with the literature [45]. After e-beam process, patterned vanadium oxide stripes (width range from 20 to 10 μm) were analyzed by Raman spectroscopy. As shown in figure 9, the peak at 192 cm^{-1} was observed at lower intensity compared to the patterned stripes. The intensity variation between the stripes and VO_2 thin film for bands at 192 cm^{-1} may be due to differences in vanadium oxide crystal orientations. The Raman peak at 442 cm^{-1} which was

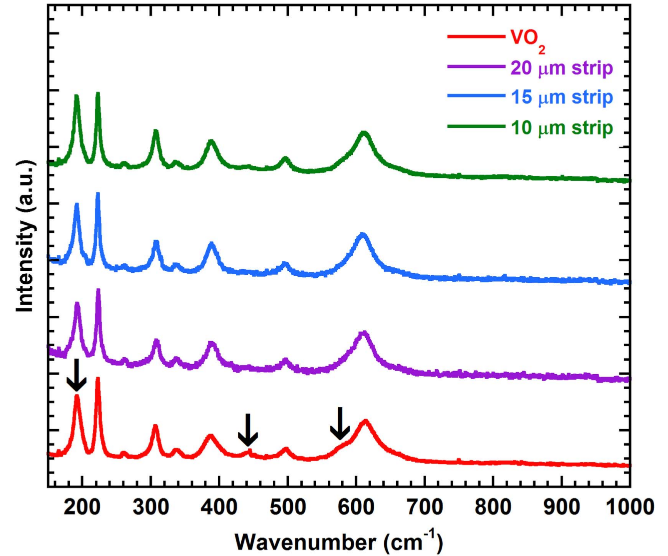

Figure 9. Raman spectrum of VO_2 and patterned vanadium oxide stripes (width range from 20 to 10 μm).

observed for VO_2 film was vanished for all patterned vanadium oxide stripes. According to Raman analysis of VO_2 film, there is a shoulder located at around 580 cm^{-1}. This shoulder was vanished in Raman analysis of patterned vanadium oxide stripes. These results show that not only variation of crystal orientation but also weaker crystalline properties occurred due to the e-beam exposure. Raman studies are also in agreement with the electrical measurements given in figure 8. It can be seen that the resistivity drops in the stripes at room temperature support that the secondary phases occurred in e-beam patterned structures. Therefore, it can be concluded that the obtained crystal structure variations are caused by e-beam patterning of stripes.

4. Conclusion

In summary, we have obtained high quality DC magnetron sputtered VO_2 thin films on c-cut sapphire substrate. Various oxygen concentrations were performed and optimized to obtain VO_2 films with a sharp resistivity drop across MIT. The change in resistivity at transition temperature of VO_2 thin film is around by a factor of 10^4, and it is convenient for electrical switching applications. Moreover, the grown VO_2 thin films exhibit nearly 50% transmission change in near-IR region, which is promising for optical applications, such as thermochromic windows.

The grown VO_2 films having 10^4 resistivity drop were used for the electrical characterization of patterned stripes. For these measurements, e-beam lithography and Ar ion etching processes were used for the purpose of patterning the grown VO_2 films in the form of stripes. As a result, we have investigated the effect of e-beam patterning on MIT characteristics of VO_2 films when the electrical characteristics of the stripes and square samples are compared. It is observed that T_{MIT} shifts close to room temperature after patterning the VO_2 films by e-beam lithography. E-beam causes a change in oxygen concentration of grown VO_2

thin film (figure 8), the metallic phase of vanadium oxide compounds becomes dominant. Secondary phases of VO_x might originate from low oxygen concentration due to local heating under high vacuum. Formed metallic phase of the secondary phase in VO_x causes a drop of resistivity of the film at room temperature while the degradation of ideal oxygen concentration leads to a decrease in the ratio of resistivity values (MIT rate) at 30 °C–90 °C. Lastly, the change in resistivity of the VO_2 stripes is an order of magnitude, and transition temperature shifts from 68 °C to 50 °C. Shifting T_{MIT} to a closer region of room temperature might be important in terms of many applications, such as thermochromic windows and bolometers.

Acknowledgments

This research is partially supported by TUBITAK (The Scientific and Technological Research Council of Turkey) with the project number 113F349 and partially by the University Research Foundation (BAP) with the project number of 2015-IYTE-42. Additionally, we thank to Applied Quantum Research Center (AQUREC) of IZTECH for the research facilities offered us with this study.

References

[1] Balu R and Ashrit P V 2008 *Appl. Phys. Lett.* **92** 21904
[2] Gopalakrishnan G, Ruzmetov D and Ramanathan S 2009 *J. Mater. Sci.* **44** 5345
[3] Nag J, Payzant E A, More K L and Haglund R F Jr 2011 *Appl. Phys. Lett.* **98** 251916
[4] Nagashima K, Yanagida T, Tanaka H and Kawai T 2007 *J. Appl. Phys.* **101** 26103
[5] Fillingham P J 1967 *J. Appl. Phys.* **38** 4823
[6] Guiton B S, Gu Q, Prieto A L, Gudiksen M S, Park H and Amer J 2005 *Chem. Soc* **127** 498
[7] Liu K, Cheng C, Suh J, Tang-Kong R, Fu D, Lee S, Zhou J, Chua L O and Wu J 2014 *Adv. Mater.* **26** 1746
[8] Yi X, Chen C, Liu L, Wang Y, Xiong B, Wang H and Chen S 2003 *Infrared Phys. Technol.* **44** 137
[9] Imada M, Fujimori A and Tokura Y 1998 *Rev. Mod. Phys.* **70** 1039
[10] Donev E U, Lopez R, Feldman L C and Haglund R F 2009 *Nano Lett.* **9** 702
[11] Goodenough J B 1971 *J. Solid State Chem.* **3** 490
[12] Krammer A, Magrez A, Vitale W A, Jeanneret P, Guibert E, Whitlow H J, Ionescu A M and Schüler A 2017 *J. Appl. Phys.* **122** 045304
[13] Gupta A, Singhal R, Narayan J and Avasthi D K 2011 *J. Mater. Res.* **26** 2901
[14] Wu J M and Liou L B 2011 *J. Mater. Chem.* **21** 5499
[15] Jiang M, Cao X, Bao S, Zhou H and Jin P 2014 *Thin Solid Films* **562** 314
[16] Yuce H 2015 *MS Thesis* Izmir Institute of Technology (http://hdl.handle.net/11147/4585)
[17] Ruzmetov D, Gopalakrishnan G, Deng J, Narayanamurti V and Ramanathan S 2009 *J. Appl. Phys.* **106** 83702
[18] Kato K, Song P K, Odaka H and Shigesato Y 2003 *Japan. J. Appl. Phys.* **42** 6523
[19] Cui H N, Teixeira V, Meng L J, Wang R, Gao J Y and Fortunato E 2008 *Thin Solid Films* **516** 1484
[20] Dicken M J, Aydin K, Pryce I M, Sweatlock L A, Boyd E M, Walavalkar S and Atwater H A 2009 *Opt. Express* **17** 18330
[21] Chen C, Yi X, Zhao X and Xiong B 2001 *Sensors Actuators* A **90** 212
[22] Gauntt B D, Dickey E C and Horn M W 2009 *J. Mater. Res.* **24** 1590
[23] Fieldhouse N, Pursel S M, Horn M W and Bharadwaja S 2009 *J. Phys. D: Appl. Phys* **42** 055408
[24] Alaboz H, Demirhan Y, Yuce H, Aygun G and Ozyuzer L 2017 *Opt. Quantum Electron.* **49** 238
[25] Stefanovich G, Pergament A and Stefanovich D 2000 *J. Phys.: Condens. Matter* **12** 8837
[26] Ruzmetov D, Gopalakrishnan G, Ko C, Narayanamurti V and Ramanathan S 2010 *J. Appl. Phys.* **107** 114516
[27] Narayan J and Bhosle V 2006 *J. Appl. Phys.* **100** 103524
[28] Kim D and Kwok H 1994 *Appl. Phys. Lett.* **65** 3188
[29] Maruyama T and Ikuta Y 1993 *J. Mater. Sci.* **28** 5073
[30] Dagur P, Mane A U and Shivashankar S 2005 *J. Cryst. Growth* **275** 1223
[31] Mousavi M, Kompany A, Shahtahmasebi N and Bagheri-Mohagheghi M-M 2013 *Phys. Scr.* **88** 6
[32] Yoon J, Kim H, Mun B S, Park C and Ju H 2016 *J. Appl. Phys.* **119** 124503
[33] Partlow D, Gurkovich S, Radford K and Denes L 1991 *J. Appl. Phys.* **70** 443
[34] Li S Y, Namura K, Suzuki M, Niklasson G A and Granqvist C G 2013 *J. Appl. Phys.* **114** 033516
[35] Kusano E, Theil J and Thornton J A 1988 *J. Vac. Sci. Technol.* A **6** 1663
[36] Shigesato Y, Enomoto M and Odaka H 2000 *Japan. J. Appl. Phys.* **39** 6016
[37] Youn D H, Kim H T, Chae B G, Hwang Y J, Lee J W, Maeng S L and Kang K Y 2004 *J. Vac. Sci. Technol.* A **22** 719
[38] Tuna O, Selamet Y, Aygun G and Ozyuzer L 2010 *J. Phys. D: Appl. Phys* **43** 055402
[39] Ozdemir M, Kurt M, Ozyuzer L and Aygun G 2016 *Eur. Phys. J. Appl. Phys.* **75** 30401
[40] Turkoglu F, Koseoglu H, Demirhan Y, Ozyuzer L, Preu S, Malzer S and Kadowaki K 2012 *Supercond. Sci. Technol.* **25** 125004
[41] Demirhan Y, Saglam H, Turkoglu F, Alaboz H, Ozyuzer L, Miyakawa N and Kadowaki K 2015 *Vacuum* B **120** 89
[42] Zhang H, Wu Z, He Q and Jiang Y 2013 *Appl. Surf. Sci.* **277** 218
[43] Luo Y, Zhu L, Zhang Y, Pan S, Xu S, Liu M and Li G 2013 *J. Appl. Phys.* **113** 183520
[44] Zhu N-W, Hu M, Xia X-X, Wei X-Y and Liang J-R 2014 *Chin. Phys.* B **23** 048108
[45] Zhao Y, Lee J H, Zhu Y, Nazari M, Chen C, Wang H and Fan Z 2012 *J. Appl. Phys.* **111** 053533
[46] Piccirillo C, Binions R and Parkin I P 2007 *Chem. Vapor Depos.* **13** 145
[47] Öksüzoğlu R M, Bilgiç P, Yıldırım M and Deniz O 2013 *Opt. Laser Technol.* **48** 102
[48] Son L N, Tachiki T and Uchida T 2011 *Japan. J. Appl. Phys.* **50** 025803
[49] Ruzmetov D, Zawilski K T, Narayanamurti V and Ramanathan S 2007 *J. Appl. Phys.* **102** 113715
[50] Tashman J W *et al* 2014 *Appl. Phys. Lett.* **104** 063104
[51] Berglund C and Guggenheim H 1969 *Phys. Rev.* **185** 1022
[52] Gurvitch M, Luryi S, Polyakov A and Shabalov A 2009 *J. Appl. Phys.* **106** 104504
[53] Wu C, Feng F and Xie Y 2013 *Chem. Soc. Rev.* **42** 5157
[54] Eguchi R, Yokoya T, Kiss T, Ueda Y, Tajima H, Yamazaki J and Shin S 2002 *Physica* B **312** 600
[55] Yamin T, Havdala T and Sharoni A 2014 *Mater. Res. Express* **1** 046302